Title: Host density has limited effects on pathogen invasion, disease-induced declines, and within-host infection dynamics across a landscape of disease

Authors: Mark Q. Wilber[1], Roland A. Knapp[2,3], Thomas C. Smith[2,3], Cheryl J. Briggs[4]

[1]Department of Forestry, Wildlife, and Fisheries, University of Tennessee Institute of Agriculture, Knoxville, TN, 37996, United States
[2]Earth Research Institute, University of California, Santa Barbara, CA, 93106, United States
[3]Sierra Nevada Aquatic Research Laboratory, University of California, Mammoth Lakes, CA, 93546, United States
[4]Ecology, Evolution and Marine Biology, University of California, Santa Barbara, Santa Barbara, CA, 93106, United States

Corresponding author: Mark Q. Wilber, mwilber@utk.edu

Abstract

1. Host density is hypothesized to be a major driver of variability in the responses and outcomes of wildlife populations following pathogen invasion. While the effects of host density on pathogen transmission have been extensively studied, these studies are dominated by theoretical analyses and small-scale experiments. This focus leads to an incomplete picture regarding how host density drives observed variability in disease outcomes in the field.

2. Here, we leveraged a dataset of hundreds of replicate amphibian populations that varied by orders of magnitude in host density. We used these data to test the effects of host density on three outcomes following the arrival of the amphibian-killing fungal pathogen *Batrachochytrium dendrobatidis* (*Bd*): the probability that *Bd* successfully invaded a host population and led to a pathogen outbreak, the magnitude of the host population-level decline following an outbreak, and within-host infection dynamics that drive population-level outcomes in amphibian-pathogen systems.

3. Based on previous small-scale transmission experiments, we expected that populations with higher densities would be more likely to experience *Bd* outbreaks and would suffer larger proportional declines following outbreaks. To test these predictions, we developed and fitted a Hidden Markov Model that accounted for imperfectly observed disease outbreak states in the amphibian populations we surveyed.

4. Contrary to our predictions, we found minimal effects of host density on the probability of successful *Bd* invasion, the magnitude of population decline following *Bd* invasion, and the dynamics of within-host infection intensity. Environmental conditions, such as summer temperature, winter severity, and the presence of pathogen reservoirs, were more predictive of variability in disease outcomes.

5. Our results highlight the limitations of extrapolating findings from small-scale transmission experiments to observed disease trajectories in the field and provide strong evidence that variability in host density does not necessarily drive variability in host population responses following pathogen arrival. In an applied context, we show that feedbacks between host density and disease will not necessarily affect the success of reintroduction efforts in amphibian-*Bd* systems of conservation concern.

Keywords: transmission; disease-induced extinction; density-dependent; frequency-dependent; *Batrachochytrium dendrobatidis*; *Rana muscosa*; *Rana sierrae*; chytridiomycosis

Introduction

A central question in disease ecology is why host populations experience different responses and outcomes following the arrival of a pathogen (Deredec & Courchamp 2003; Lloyd-Smith *et al.* 2005; Davis *et al.* 2007; Frick *et al.* 2017; Golas *et al.* 2021). Observed variability in population responses and outcomes following pathogen arrival (henceforth "response trajectories") depends on at least five different branch points (Fig. 1; Wilber *et al.* 2019). The first branch point determines whether a pathogen successfully invades the host population (Diekmann *et al.* 2013). The second determines the effect of a pathogen on the host population (negative, positive, or no effect; Tompkins *et al.* 2011). The third determines whether a population that has experienced disease-induced declines experiences disease-induced extinction or continues to persist at low densities with or without the pathogen (De Castro & Bolker 2005). The fourth determines whether a host population that has been reduced in size by infection persists or experiences stochastic extinction (Golas *et al.* 2021). Finally, the fifth determines whether the population starts to recover towards a pre-invasion population size with or without the pathogen (Golas *et al.* 2021). These branch points encompass a rich set of theory on host suppression, resilience, stability, and stochasticity and provide a tractable way to uncover potential factors driving the observed variability in response trajectories in host-pathogen systems. However, for wildlife disease systems in particular, we rarely have field data of sufficient temporal resolution across replicate populations to examine the mechanisms driving outcomes at more than one branch point along a response trajectory (Davis *et al.* 2007; Frick *et al.* 2017; Dallas *et al.* 2018, but see Reijniers *et al.* (2012)). This omission leads to an incomplete picture regarding the key mechanisms driving observed variability in response trajectories and how the role of these mechanisms can change over the course of an outbreak.

Host density is a central characteristic that can affect multiple branch points of response trajectories (Anderson & May 1979; Davis *et al.* 2007; Reijniers *et al.* 2012). Host density affects pathogen transmission if the between-host contact rate increases with host density over at least some range of host densities (Hopkins *et al.* 2020). Epidemiologically, the relationship between host density and transmission rate directly affects the ability of a pathogen to successfully invade a host population (branch point 1) (Lloyd-Smith *et al.* 2005), the magnitude of disease-induced declines following invasion (branch point 2) (Diekmann *et al.* 2013), and the propensity for disease-induced extinction (branch point 3) (De Castro & Bolker 2005). Ecologically, the effects of demographic stochasticity – the probabilistic nature of births and deaths – on population persistence are the strongest in small populations and can result in population extirpation following disease-induced declines even if the pathogen does not directly drive the host population extinct (branch point 4) (Lande *et al.* 2003). Thus, elucidating the effects of host density on various branch points is important to describe variability in response trajectories in host-parasite systems. However, many studies either i) focus on the effects of density on transmission in small-scale experiments and then extrapolate these effects up to natural populations (Dallas *et al.* 2018; Tompros *et al.* 2022) or ii) focus on the effects of density at a single branch point in the field (e.g., pathogen invasion, Davis *et al.* 2007), even though the effects of host density can vary across the response trajectory (Begon *et al.* 2019). Given the potential importance of host density for the invasion and persistence of pathogens in host populations (Deredec & Courchamp 2003; Hopkins *et al.* 2020), the impact of density on each (or all) branch points along a response trajectory in actual field settings remains a key knowledge gap in most wildlife disease systems. This gap is particularly important for host species of conservation concern, where the multifaceted role of density across response trajectories can inform a wide range of species recovery actions, including optimal reintroduction strategies (Aiello *et al.* 2014).

The amphibian species complex *Rana muscosa* and *Rana sierrae* provides an ideal system to test how host density affects response trajectories following the arrival of the fungal pathogen *Batrachochytrium dendrobatidis* (*Bd*). Henceforth, we refer to both species as *R. sierrae* as there are few known epidemiological or ecological differences between the species. *R. sierrae* live in high elevation lakes and streams in California's Sierra Nevada mountains, constituting hundreds of largely independent populations on the landscape (Knapp & Matthews 2000). *Bd* has successfully invaded nearly all these populations over the last fifty years (Knapp *et al.* 2016; Vredenburg *et al.* 2019). Aquatic *Bd* zoospores infect the skin of amphibian hosts where they form sporangia and produce additional zoospores that can re-infect the same host and lead to increasing *Bd* infection intensity (Longcore *et al.* 1999; DiRenzo *et al.* 2018). Extensive surveillance of frog populations and disease presence in hundreds of waterbodies over 25 years has documented the following response trajectories in populations of *R. sierrae* (Briggs *et al.* 2010; Jani *et al.* 2017): 1) *Bd* is detected in a previously naive population and either sparks or fails to spark an epizootic, 2) if an epizootic occurs, the intensity of *Bd* infection on hosts increases rapidly, leading to host death and population-level decline (Vredenburg *et al.* 2010), 3) infected host populations either continue to decline until extirpation or persist at reduced density with ongoing *Bd* infection (Briggs *et al.* 2010), and 4) some amphibian populations eventually begin to recover despite the continuing presence of *Bd* (Knapp *et al.* 2016; Joseph & Knapp 2018). Moreover, a previous small-scale transmission experiment found that *Bd* transmission depends on *R. sierrae* density directly through host contacts (standard density-dependent transmission) and indirectly through the density of *Bd* zoospores in the water (Wilber *et al.* 2017). We have the opportunity to combine data from hundreds of populations across a gradient of host densities and disease outcomes with predictions from transmission experiments to ask: How does host density affect *R. sierrae*-*Bd* response trajectories following *Bd* arrival?

The intrinsic reproductive number R_0 provides a theoretical framework for answering this question. The quantity R_0 describes the average number of infections produced by an average infected individual in a fully susceptible population and relates directly to population-level outcomes such as pathogen invasion and the size of epizootics (Diekmann *et al.* 2013). Given previously observed density-dependent transmission in mesocosm experiments (Wilber *et al.* 2017), R_0 is expected to be proportional to host density in the *R. sierrae*-*Bd* system. However, host density is one of multiple factors that can affect response trajectories. For example, in this system the magnitude of *Bd*-induced declines is correlated with *Bd* infection intensity (Vredenburg *et al.* 2010) which can be modulated by temperature (Andre *et al.* 2008). Thus, host populations with similar host densities may still experience different response trajectories following the arrival of a pathogen if environmental conditions such as temperature (Kilpatrick *et al.* 2010; Sonn *et al.* 2019) affect infection intensity.

Here, we test three hypotheses regarding how host density and infection intensity drive variability in response trajectories. First, we predict that higher host density should increase the probability of successful *Bd* invasion into an *R. sierrae* population, resulting in an epizootic (branch point 1, Fig. 1). Given density-dependent transmission, increasing host density should increase R_0 and increase the probability of successful invasion (and alternatively, decrease the probability of failed invasion) (Lloyd-Smith *et al.* 2005; Diekmann *et al.* 2013). Second, given density-dependent transmission, the magnitude of population decline given disease invasion should increase with increasing R_0 (Fisher *et al.* 2012; Diekmann *et al.* 2013). We therefore predict that the magnitude of host population declines following *Bd* invasion should increase for higher host population density prior to decline (branch point 2-4). Finally, while it is often assumed that the accumulation of *Bd* infection intensity following initial infection is driven by within-host processes and is largely decoupled from the density of hosts in the environment (Wilber *et al.* 2017; DiRenzo *et al.* 2018), there is some evidence that host density can influence chytrid infection intensity (Bosch *et al.* 2020; Tompros *et al.* 2022). We test this hypothesis and predict that host density in enzootic and epizootic scenarios will not have a clear effect on *Bd* infection intensity (branch point 2).

Materials and methods

Field sites and data collection

During the period 2004-2019, we conducted surveys of the lakes and ponds in Yosemite, Sequoia, and Kings Canyon National Parks, California, USA that harbored most of the known *R. sierrae* populations (Knapp *et al.* 2003; Knapp 2005). In Sequoia and Kings Canyon, the objective of these surveys was to describe the ongoing spread of *Bd* through *R. sierrae* populations (Vredenburg *et al.* 2010; Zhou *et al.* 2015). In Yosemite, where *Bd* is essentially ubiquitous and has been present for several decades (Vredenburg *et al.* 2019), the objective was to describe the status of *Bd*-infected frog populations and frog-*Bd* dynamics (Knapp *et al.* 2011, 2016). At each water body, counts of *R. sierrae* adults, subadults, and tadpoles were made during diurnal visual encounter surveys (VES) of the entire water body shoreline and the first 100m of inlet and outlet streams. During the summer, adults, subadults, and tadpoles occur almost exclusively in shallow water near shore and are easily detected, and counts are highly repeatable (Knapp & Matthews 2000). Following VES, we collected skin and mouthpart swabs from frogs and tadpoles to quantify *Bd* infection intensities (Boyle *et al.* 2004). Although we targeted the collection of swabs from up to 20 individuals per site-survey, constraints associated with limited time, adverse weather conditions, and small population size often resulted in the collection of fewer swabs. Skin swabs were analyzed using standard *Bd* DNA extraction and qPCR methods (Boyle *et al.* 2004, for *R. sierrae*-specific details see Joseph & Knapp (2018)).

From 2004-2019 we surveyed a total of 956 total lakes and ponds surveyed at least once for either frog abundance or *Bd*, for a total of 3,168 unique lake × year surveys. Not all lakes were visited in all years due to their remoteness (e.g., many lakes were $>$ 10 miles from the nearest road). A total of 449 lakes were surveyed in three or more years from 2004-2019. For the three analyses subsequently described, we used different subsets of this dataset. Field work was conducted under an Institutional Animal Care and Use Committee (IACUC) permit at the University of California Santa Barbara (# 478). Field permits for sampling included YOSE-2015-SC1-0047, YOSE-2016-SC1-0121, YOSE-2017-SC1-0109, YOSE-2018-SC1-0027, and YOSE-2019-SC1-0025 from Yosemite National Park and TE40090B from the US Fish and Wildlife Service.

Hypothesis 1: Higher amphibian density increases the probability of a successful *Bd* invasion

We used a multi-state *Bd* occupancy model to test whether lakes with higher host density had higher probabilities of successful *Bd* invasion than lakes with lower host densities. In a fully susceptible population with $R_0 > 1$, a pathogen can still fail to spark a large outbreak following its arrival (Diekmann *et al.* 2013). Qualitatively, this might manifest as the pathogen appearing in the population, being detected at low prevalence for some period of time, and then disappearing. We characterize this qualitative behavior as a failed invasion. Alternatively, a pathogen could i) arrive in the population and remain at low prevalence for some time before eventually increasing in prevalence or ii) immediately increase in prevalence upon arrival. We consider both of these behaviors as a successful invasion. Once *Bd* successfully invades in this system, *R. sierrae* populations consistently show high prevalence and infection intensity (Briggs *et al.* 2010; Vredenburg *et al.* 2010). We designed a multi-state *Bd* occupancy model to capture these behaviors related to failed and successful invasion. Here, we give a brief overview of this model and provide a complete description in Appendix S1.

The state process model

Consider a frog population in lake j sampled at year t, where t to $t+1$ refers to June in one year to June in the following year. We assume that a frog population can occupy four potential states (Fig. 2). First, the population j at time t can be truly *Bd*-free, denoted as $X_{U,j,t}$, where 'U' indicates 'Unoccupied by *Bd*'. Second, the population j can be *Bd*-positive, but *Bd* is present in the population below some prevalence ρ. We denote this state at $X_{LP,j,t}$, where 'LP' indicates 'low prevalence'. Third, the population j can be infected with *Bd* above some prevalence ρ, denoted as $X_{HP,j,t}$ where 'HP' indicates 'high prevalence'. Finally, as is the case in the *R. sierrae* system, frog populations can also be extirpated by *Bd*, denoted as $X_{E,j,t}$. We model transitions among these four states in population j as described in Fig. 2.

To test our hypothesis regarding failed and successful invasions, we focused on two parameters: $\varphi_{j,t}$ and $\omega_{j,t}$. Given that *Bd* arrives in a population, the parameter $\omega_{j,t}$ determines the probability of transitioning to low prevalence or immediately experiencing a successful invasion and transitioning to high prevalence $(1-\omega_{j,t})$. Similarly, the parameter $\omega_{j,t}$ also defines the probability that a population in a low prevalence state remains in a low prevalence state and does not experience a successful invasion in a subsequent year. The parameter $\varphi_{j,t}$ gives the probability of population j in a low prevalence state transitioning back to a *Bd*-free state and experiencing a failed invasion in a subsequent year. We assume that $\varphi_{j,t}$ and $\omega_{j,t}$ only depend on the current state and covariates (i.e., the Markov property). Note that a complete failed or successful trajectory given *Bd* arrival is a combination of parameters $\varphi_{j,t}$ and $\omega_{j,t}$ (higher values of $\varphi_{j,t}$ and $\omega_{j,t}$ signify increased tendency for failed invasions).

Covariates affecting successful and failed invasions

We tested how host density and abundance of population j at time t affected $\varphi_{j,t}$ and $\omega_{j,t}$ and thus affected failed and successful invasions. In addition to host density, we also included three covariates that could affect failed or successful invasion: maximum summer temperature, winter severity, and tadpole presence/absence (Andre *et al.* 2008; Briggs *et al.* 2010; Joseph & Knapp 2018). Using gridMET (Abatzoglou 2013), we extracted the mean maximum air temperature at the location of population j in year t for the period June-September, which are the months that frogs are active in the Sierra Nevada. Lab experiments have shown that temperature affects infection intensity and frog survival in this system (Andre *et al.* 2008; Wilber *et al.* 2016) and thus may impact failed or successful *Bd* invasion at finer temporal timescales than tested previously (e.g., Knapp *et al.* 2011).

Water temperature may be a more important driver of frog-*Bd* dynamics than air temperature for the highly aquatic *R. sierrae*. Temperature of Sierra Nevada water bodies is heavily influenced by winter severity. The high elevation lakes that *R. sierrae* inhabit are under ice and snow cover from approximately November-June. More severe winters lead to longer ice and snow cover, shorter ice-free durations during summer months, and cooler summer water temperatures (Smits *et al.* 2021). A well-supported measure/proxy of winter severity is the snow water equivalent (SWE) on April 1st of the current year (extracted from the California Data Exchange Center for snow survey locations across the Sierra Nevada). We used April 1 SWE as a predictor of failed or successful *Bd* invasion. As our measure of winter severity temporally followed maximum summer temperature (e.g., maximum summer temperature in summer 2009 followed by snow water equivalent measured in April 1 of 2010), we also included an interaction to test whether winter severity modulated the effect of summer temperature on failed invasions.

Finally, tadpoles can act as an important reservoir for *Bd* in this system, maintaining infection but not suffering disease-induced mortality (Briggs *et al.* 2010). We expected that the presence of tadpoles would increase the persistence of *Bd* and decrease the probability of a failed invasion.

We modeled $\varphi_{j,t}$ and $\omega_{j,t}$ as

$$\begin{aligned}\text{probit}(\cdot_{j,t}) =& \beta_{\cdot,0} + \beta_{\cdot,1}\log_{10}(D_{j,t}) + \beta_{\cdot,2}(\text{Max. summer temperature}_{j,t}) + \beta_{\cdot,3}(\text{Winter severity}_{j,t}) + \\ & \beta_{\cdot,4}(\text{Tadpole presence}_{j,t}) + \beta_{\cdot,5}(\text{Max. summer temperature}_{j,t} \times \text{Winter severity}_{j,t})\end{aligned} \tag{1}$$

where 'probit' indicates the probit link function (the inverse cumulative density function of a standard normal distribution) and $\cdot$ refers to either φ or ω. The variable $D_{j,t}$ is either the observed abundance of adult and sub-adult *R. sierrae* in population j in year t based on VES or the density of *R. sierrae* (abundance in population j at time t / perimeter of lake j). Our primary hypothesis was that increasing $D_{j,t}$ would decrease $\varphi_{j,t}$ and $\omega_{j,t}$.

We also considered three additional models with different covariates as described in Table 1. We describe how we account for missing covariates in Appendix S2.

The observation process model

Let $Y_{j,t}$ be the observed state of population j at year t. When $Y_{j,t} = U$, *Bd* was not observed in a population. When $Y_{j,t} = LP$, observed *Bd* prevalence was equal to or below the threshold ρ and the population was classified as low prevalence. When $Y_{j,t} = HP$, observed *Bd* prevalence was above the threshold ρ and the population was classified as high prevalence. When fitting the model, we varied this cutoff ρ between 0.25-0.5 to assess its influence on our results. Finally, when $Y_{j,t} = E$, no subadults or adults were observed after

Bd-induced declines and the population was classified as extirpated. Given the long-lived tadpole stage of this species (up to three years) and their resistance to *Bd*-induced mortality, tadpoles may still have been present in the population after adult and subadult extirpation. We have observed no population recovery when only tadpoles persist following an outbreak and classify these populations as functionally extirpated, E.

The probability of correctly classifying a population as *Bd*-free (U), low prevalence (LP), or high prevalence (HP) depends on how many frogs were sampled for *Bd* in the population and the unknown true *Bd* prevalence on frogs. We directly accounted for this source of observation error as described in Appendix S1.

Data selection

To examine the effects of host density on failed *Bd* invasion, we identified frog populations that we surveyed prior to *Bd*-induced declines. First, we included populations where *Bd* was not observed on the first survey but was then subsequently observed in later surveys. Second, we also included populations where *Bd* was detected on the first survey, but was then not detected on the next survey given at least five *Bd* swabs were obtained and given that the population did not undergo *Bd*-induced declines over the interval between the first and second survey. Finally, we excluded populations where frogs were reintroduced to the location as part of ongoing amphibian recovery efforts, populations that had fewer than three *Bd* swabbing visits from 2004-2019, and all populations from Yosemite National Park where *Bd* invaded prior to the onset of *Bd* sampling in 2004 (Vredenburg *et al.* 2019). In total, we used 79 populations sampled over 16 years in this analysis. Figure 2B shows representative trajectories for 16 of these populations.

Model fitting

To fit our model to the data, we used the forward algorithm to combine the state process and the observation process to estimate the likelihood of an observed sequence of states $\mathbf{y}_{j,\cdot} = \mathbf{y}_{j,1}, \mathbf{y}_{j,2}, \ldots, \mathbf{y}_{j,n}$ for population j (Appendix S1; McClintock *et al.* 2020). $\mathbf{y}_{j,t}$ is a zero-one vector (i.e., an indicator) specifying whether the observed state of population j at time t was either $[Bd\text{-free}, \text{Low prevalence}, \text{High prevalence}, \text{Extirpated}]$. We implemented all models in Stan (Carpenter *et al.* 2017). We performed structural model comparison using Pareto smoothed leave-one-out information criterion (LOOIC; Vehtari *et al.* 2016; Merkle & Rosseel 2018), where lower values indicate better out-of-sample performance. We also tested for the role of sampling bias as lakes with higher frog abundance tended to have more animals swabbed (Appendix S3).

Hypothesis 2: Higher pre-invasion amphibian density increases the magnitude of disease-induced declines

To test this hypothesis, we first identified populations that likely had not experienced *Bd* epizootics or declines at the beginning of our sampling in 2004, but had experienced successful *Bd* invasion by the end of our sampling in 2019. To identify these populations, we first only considered populations in the eastern portion of Sequoia and Kings Canyon National Parks, as these populations had generally not experienced *Bd*-induced declines prior to the start of our surveys in 2004. Because this analysis relied on estimates of proportional changes in frog abundance, we then excluded populations that had fewer than three visual encounter surveys or swabbing events from 2004-2019. Of these lakes, we then identified the maximum and minimum frog abundances that were observed from 2004-2019, the years these maximum and minimum abundances were observed, and the maximum *Bd* prevalence experienced by the population. We included populations where i) maximum observed frog abundance occurred prior to minimum frog abundance and ii) maximum prevalence was greater than 0.25 and occurred between maximum and minimum observed adult abundance. The first criterion ensured we included populations that at least experienced some decline. The second criteria ensured that *Bd* prevalence peaked between observed maximum and minimum abundance and helped identify populations where *Bd* successfully invaded and at least partially contributed to observed declines.

We examined two metrics of frog abundance. First, we counted both adults and subadults toward the total frog abundance and *Bd* prevalence. Our rationale was that the abundance of subadults prior to *Bd* invasion would contribute to R_0 and the magnitude of declines. However, our measure of subadult abundance is subject to more variability than adult abundance. Thus, we also considered a dataset where only adult frogs contributed to abundance and *Bd* prevalence. The adult and subadult dataset contained 82 populations that met the criteria described above and the adult-only dataset contained 52 populations.

We then asked: Is amphibian abundance or density prior to decline in a population predictive of the magnitude of the population decline following *Bd* invasion? Given density-dependent transmission, epidemiological theory predicts that the final size of an epizootic (one minus the proportion of susceptible hosts remaining in the population after an epizootic has concluded) is directly related to the intrinsic reproductive number R_0, which in turn depends on host density (Fisher *et al.* 2012; Diekmann *et al.* 2013). Thus, we expected that increasing host abundance or density should increase R_0 and increase the final size of the epizootic.

We used a Beta-binomial regression where our response variable was the minimum abundance of the frog population in lake j, $n_{\text{minimum abundance},j}$. Our model was

$$\begin{aligned} n_{\text{minimum abundance},j} &\sim \text{Beta-Binomial}(n_{\text{pre-decline abundance},j}, p_{\text{decline},j}, k) \\ \text{logit}(p_{\text{decline},j}) &= \beta_0 + \beta_1 \log_{10}(D_j) \end{aligned} \tag{2}$$

where the variable $p_{\text{decline},j}$ is the expected proportion population decline in lake j and k is the shape parameter of the Beta-binomial distribution. The covariate D_j is either pre-decline frog abundance in lake j $n_{\text{pre-decline abundance},j}$ or density $n_{\text{pre-decline density},j} = n_{\text{pre-decline abundance},j}/\text{lake perimeter}_j$.

We standardized the density covariates before fitting the model (subtracted the mean and divided by the standard deviation). We fit the model with a Bayesian approach using Stan (Carpenter *et al.* 2017) and put slightly regularizing priors on the non-intercept coefficients of $\text{Normal}(0, \sigma = 5)$. We used an uninformative prior on the intercept β_0.

Hypothesis 3: Amphibian density does not affect within-host infection dynamics

To test for the effect of host density on *Bd* infection load, we performed two analyses. In the first analysis, we used a subset of the data that included populations where hosts were persisting enzootically and potentially recovering in the presence of *Bd*. These consisted of 111 data points from 40 populations located in Yosemite National Park where *Bd* invasion and declines occurred prior to 2004 (the onset of our sampling, Knapp *et al.* 2016; Vredenburg *et al.* 2019). Focusing on enzootic populations allowed us to eliminate the potential causal pathway from *Bd* infection intensity to host density in a time step and isolate whether there was evidence for a causal pathway between host density and *Bd* infection intensity. We fit a piece-wise, linear regression consistent with the causal diagram in Fig. S3. This amounted to fitting two linear regressions: one where *Bd* load in the current year was predicted by *Bd* load in the previous year and amphibian density in the current year and the other where amphibian density in the current year was predicted by *Bd* load in the previous year. We were interested in whether the path coefficient (i.e., standardized regression coefficient) between host abundance or density and *Bd* load at time t was clearly distinguishable from zero.

In the second analysis, we tested the role of host density on within-host infection dynamics during an epizootic. We examined whether the within-host infection dynamics of individuals collected from a population experiencing an epizootic and released into lakes containing no frogs (i.e., low density) were similar to the infection dynamics within the more dense donor population. We used opportunistically-collected data from a conservation action where 120 adult frogs existing in a lake containing nearly 800 adult frogs were translocated to three frog-free lakes (40 per lake) in an effort to reestablish frog populations at these sites. As described in detail in Appendix S4, this translocation occurred concurrent with the onset of an epizootic in the donor population and translocated populations, providing an unfortunate but rare opportunity to quantify the effect of frog density on within-host infection dynamics.

We tested whether final *Bd* infection intensity was different between frogs in the three translocated populations in low abundance/density environments and donor frogs in a high abundance/density environment approximately one month following translocation. For all populations, frogs started with an infection intensity near zero. Our hypothesis was that infection intensities in the low abundance translocated populations would not be systematically lower or higher than infection intensities in the high abundance donor population. We fit linear models where log *Bd* infection intensity was our normally distributed response variable and lake ID (one donor lake and three translocated lakes) was our predictor variable. We allowed the variability in infection intensity to differ among lakes. We compared models using LOOIC and used uninformative priors on our model parameters over their range of support.

Results

Higher amphibian density has little effect on the probability of failed or successful *Bd* invasions

There was little support for our predictions that higher amphibian abundance or density increased the probability of successful *Bd* invasion or decreased the probability of failed invasion (Fig. 3). For all models we explored, the probability ω of a population remaining in a low prevalence state compared to transitioning to a high prevalence state showed a trend with host abundance in the opposite direction than we expected – namely, there was some evidence that increasing frog density/abundance increased the probability of remaining in a low prevalence state (Fig. 3, Fig. 4A). This trend was not a result of sampling bias and persisted even after accounting for observation error and rarefying the data (Appendix S3; Fig. S1). The probability φ of a population transitioning from a low prevalence *Bd* state to a *Bd*-free state was not strongly associated with host abundance or density (Fig. 3, Fig. 4B).

In comparison to host density, there was a stronger effect of maximum temperature on the probability of successful vs. failed *Bd* invasion. Across the different models that we fit, increasing maximum summer air temperature in the previous year (with a range of 11-18 degrees C across sites) generally increased the probability of failed invasion in the following year (increased φ, Fig. 3, Fig. 4C-D) and decreased the probability that a population transitioned to a high prevalence state (increased ω). While our choice of ρ affected whether the 95% credible interval of the temperature coefficient included zero, the direction of the temperature effect was consistent across all of our models for both host density and abundance. Rarefying the data showed that the inferred positive effect of temperature was most robust for φ. There was little evidence for a non-linear effect of temperature on φ (Table 1).

We found evidence that the temperature effect was modified by winter severity – more severe winters reduced the positive effect of temperature on φ and ω (Fig. 3, Fig. S2A, Table 1). Rarefying the data showed that this inferred relationship was most robust for ω – namely that the probability of observing a transition from low to high prevalence in a given year was less influenced by temperature in the preceding summer if the summer was followed by a more severe winter (Fig. 3).

Finally, tadpole presence decreased probability of failed invasion – the presence of tadpoles in the previous year increased the probability that *Bd* persisted in the population to the current year (i.e., a negative effect on φ; Fig. 3, Fig. 2B). This result was consistent when we used $\log_{10}$ observed tadpole abundance as a predictor variable, though using tadpole presence/absence as a covariate led to a better predictive model (LOOIC from model with tadpole presence/absence was > 3 units lower than a model with $\log_{10}$ tadpole abundance, Table 1). In contrast, we detected little effect of tadpole presence on the probability of a population transitioning to a high prevalence state (ω).

Higher host density weakly increases the magnitude of disease-induced declines

Higher frog abundance or density prior to *Bd* invasion was weakly predictive of larger disease-induced declines (Fig. 5). When we included only adult frogs in our analysis, there was a positive trend between magnitude of decline and maximum host abundance/density prior to *Bd*-induced declines, but the 95% credible intervals overlapped zero (Fig. 5A-B). In contrast, when we considered adult and subadult abundance/density, increasing host density prior to *Bd*-induced declines increased the magnitude of declines (95% credible intervals did not overlap zero; Fig. 5C-D). However, across at least two orders of magnitude of host abundance/density, any protective effect of low density on the magnitude of decline likely had minimal biological significance. That is, even very small populations experienced large proportional declines. For example, for a population with seven individuals, our model predicted an 84% decline (95% CI: [73%, 91%]), which corresponds to approximately six of the seven individuals suffering *Bd*-induced mortality.

Higher amphibian density has little effect on infection intensity

For enzootic populations, there were small effects of host abundance or host density at time t on mean *Bd* infection load at time t (Fig. S3). The path coefficients on the link between host abundance or density in year t and *Bd* infection intensity at year t all overlapped zero (Fig. S3).

We also detected no consistent effect of host abundance on infection intensity for populations undergoing an epizootic (Fig. 6A). In our opportunistic translocation study, infection load varied among the four populations (Fig. 6B). Despite this variation, all mean infection intensities were still above 1 million ITS copies and mean infection intensities in low abundance translocated populations were not less than infection intensities in the high abundance donor population (Fig. 6B; ΔLOOIC of the model assuming lower infection intensities in translocated populations compared to the donor population - model where infection intensities were free to vary: 10.9). Rather, in two of the translocated populations (50170 and 50219), there was evidence that mean infection intensity was higher than in the donor population (Fig. 6B; difference in mean log infection intensity relative to donor population 50183: $\beta_{50170} = 0.31$, 95% credible interval: [0.03, 0.60]; $\beta_{50219} = 0.45$, 95% CI: [0.14, 0.75]). In the remaining translocated population 50194, mean infection intensity was not distinguishable from the source population (Fig. 6B; $\beta_{50194} = -0.10$, 95% CI: [-0.47, 0.26]). Combined abundance of tadpoles, subadults, and adults was orders of magnitude higher in the donor population compared to the translocated populations (Fig. 6C).

Discussion

Host density is hypothesized to be a major driver of variability in response trajectories following disease invasion in wildlife populations (Lloyd-Smith *et al.* 2005; Begon *et al.* 2019; Golas *et al.* 2021). While the effects of host density on transmission have been extensively studied in host-parasite systems (reviewed in Hopkins *et al.* 2020), these studies are dominated by theoretical analyses and small-scale experiments. Here, we leveraged a dataset consisting of hundreds of replicate amphibian populations invaded by the fungal pathogen *Bd* across 25 years to test the effects of host density and abundance (henceforth referred to as "host density" as the effects were similar) on observed variability in response trajectories. Counter to our predictions, we found minimal effects of host density on the probability of successful *Bd* invasion and the magnitude of population decline following *Bd* invasion. Moreover, we found little evidence that host density affected the dynamics of within-host infection intensity.

We expected host density to be an important factor driving variation in response trajectories for three reasons. First, we generally would expect a relationship between host density and *Bd* transmission as more frogs shed more zoospores, leading to increased infection (Briggs *et al.* 2010; Courtois *et al.* 2017). Second, a small-scale transmission experiment in this system found that density-dependent transmission better described observed *R. sierrae*-*Bd* transmission than other functions such as frequency-dependent or constant transmission (Wilber *et al.* 2017). Finally, host density is a positive predictor of *Bd* prevalence, transmission, and declines in other amphibian-*Bd* studies (Rachowicz & Briggs 2007; Gillespie *et al.* 2015; Adams *et al.* 2017). Despite these *a priori* lines of evidence, we observed little effect of host density on disease outcomes across multiple branch points of the response trajectory.

There are at least two potential explanations for this result. First, the observed density-dependent transmission for *R. sierrae* in small-scale mesocosm experiments may not be reflective of the transmission dynamics in the field. In particular, contact dynamics leading to approximate frequency-dependent transmission might be a driver of multi-year disease dynamics in this system. In the Sierra Nevada, *R. sierrae* adults and tadpoles aggregate when over-wintering under lake ice, which occurs for approximately nine months of the year (Knapp 2021). If the size of aggregations is largely independent of host density and aggregations are occurring for over 75% of year, then we might expect frequency-dependent disease dynamics to drive the response trajectories of *R. sierrae*, despite infection dynamics during summer months being more consistent with density-dependent transmission. This could also explain why small-scale transmission experiments that lasted only 32 days in the summer were not reflective of multi-year disease dynamics observed in the field (Wilber *et al.* 2017). Our results provide a sober reminder of the limitations of extrapolating small-scale, short-term transmission experiments to predict patterns in multi-year response trajectories (Mihaljevic *et al.* 2020).

The second explanation is that, even under density-dependent transmission, stochasticity in infection dynamics and the environment can mask the effects of density (Lloyd-Smith *et al.* 2005; Briggs *et al.* 2010; Kyle *et al.* 2020). For example, Briggs *et al.* (2010) developed a stochastic model of this frog-*Bd* system and showed that given only density-dependent infection dynamics one could obtain response trajectories consistent with enzootic or epizootic dynamics. These differences in response trajectories were not necessarily mediated by differences in initial host density, but by within-host infection processes such as the rate that *Bd* zoospores reinfect the same host (Briggs *et al.* 2010). Moreover, for density-dependent host-pathogen systems, demographic and environmental stochasticity can significantly blur the effects of host density on disease invasion and persistence (Lloyd-Smith *et al.* 2005; Kyle *et al.* 2020). The dataset we used here was unique in that it addressed many of the challenges identified when testing for density thresholds in wildlife pathogen systems (Lloyd-Smith *et al.* 2005): it contained hundreds of replicate populations, host abundance spanned orders of magnitude (from 10s to 1000s of individuals), and the system was largely driven by a single host species (though see Reeder *et al.* 2012). So despite the inherent challenges of stochasticity and finite populations, the *R. sierrae*-*Bd* system was uniquely poised to detect an effect of host density on successful pathogen invasion or the magnitude of host decline, if one existed.

We did detect an effect of host density on the magnitude of disease-induced declines in a direction consistent with our *a priori* predictions related to density-dependent transmission. However, the biological significance of this density effect for describing variability in response trajectories may be small as the predicted magnitude of declines for even small populations was still nearly 85%. This was further echoed in our results regarding within-host infection dynamics, where we found that regardless of host density or whether a population was in an epizootic or enzootic state, density had minimal effect on *Bd* infection intensity. Thus, lower host densities provided little meaningful protective effects for naive *R. sierrae* populations where *Bd* had successfully invaded.

In contrast to host density, we found that environmental conditions were more important factors driving disease outcomes. Given a less severe winter, higher maximum summer air temperature in the previous year increased the probability of failed invasion and reduced the probability of a population transitioning to a high prevalence state in the following year. However, winter severity's interaction with summer temperature made its overall effect on failed *Bd* invasion context-dependent. Interpreting the biological meaning of this interaction between winter severity and summer temperature remains speculative. However, we do know that winter severity can decrease infected host survival (Joseph & Knapp 2018) and exploring how and why this covariate interacts with other environmental covariates is an interesting future direction to explore. For example, the observation that cool summers and severe winters lead to a decreased probability of population transitioning to a high prevalence state could be a result of mortality bias: perhaps highly infected individuals are removed from the population over winter leading to observed failed invasions where *Bd* is at least temporarily removed from the population through host mortality.

For less severe winters, the positive effect of temperature on failed invasion probability was consistent with other amphibian-*Bd* field studies. In these previous studies, increased temperature generally decreased *Bd* prevalence and infection intensity (Sonn *et al.* 2019), which would correspondingly increase the probability of *Bd* failing to invade. Previous laboratory studies on *R. sierrae*-*Bd* interactions have identified non-linear effects of temperature on infection dynamics, with *Bd* growth rate increasing from 4 to 20 degrees C with subsequent decreases in frog survival probability (Wilber *et al.* 2016), and *R. sierrae* survival probability increasing between 20-26 degrees C, likely due to decreases in *Bd* growth rate (Andre *et al.* 2008). While these previous results might suggest that maximum mean summer air temperatures between 11-18 degrees C as observed at our field sites should increase successful *Bd* invasions, one cannot directly compare the absolute value of laboratory temperatures and air temperatures from the field. Mean air temperature from June to September is correlated with, but not the same as, temperature in the ambient environment experienced by amphibians (Bradford 1984). A useful next step will be to quantify the availability and selection of fine-scale thermal refuges and whether this provides additional explanatory power for the observed variability in response trajectories across amphibian populations (Barrile *et al.* 2021).

The presence/absence of *R. sierrae* tadpoles was also a significant predictor of the probability of failed *Bd* invasion across populations. This result is consistent with the hypothesis that tadpoles are a temporary *Bd* reservoir in this system, maintaining high levels of *Bd* infection but suffering little mortality until metamorphosis (Briggs *et al.* 2010). Interestingly, our model predicted that while tadpoles helped maintain *Bd* in a population, they had little effect on the onset of an epizootic (i.e., transitions from a low prevalence to a high prevalence state). Reservoir hosts – a group of hosts that contribute to continued infection in another group of hosts (Haydon *et al.* 2002) – can affect pathogen presence and epidemic potential in a focal group. However, when transmission (i.e., the event of becoming infected) and within-host infection processes (i.e., the increase of pathogen in the host following infection) are driven by different causes, reservoirs contributing to pathogen spillover in a focal host or lifestage might not be directly responsible for subsequent outbreaks.

Our results have important applied implications for population management in this system and other systems where pathogens are of conservation concern. Reintroductions are an important tool for re-establishing amphibian populations (Joseph & Knapp 2018; Canessa *et al.* 2019). While larger population sizes or repeated introductions are often associated with increased reintroduction success (Fischer & Lindenmayer 2000), when pathogen transmission is density-dependent, large reintroduced populations can suffer from increased transmission, more severe population declines, and lower probabilities of long-term persistence (Fisher *et al.* 2012; Aiello *et al.* 2014). We detected weak effects of host density on disease outcomes, indicating that reintroduction efforts in this system are unlikely to be limited by negative effects of large reintroductions on transmission and disease-induced declines. Rather, environmental conditions seem to play a larger role on disease outcomes (echoed in Joseph & Knapp 2018). Quantifying how host density and other population parameters or covariates affect branch points across a response trajectory provides a powerful framework to disentangle variability in disease outcomes in real populations and inform subsequent management efforts.

Acknowledgements

We thank the following for contributions to this study: Ericka E. Hegeman - project and data management, field work; A. Barbella and K. Rose - laboratory qPCR; and numerous field technicians who assisted with frog surveys (especially A. Beechan, B. Currinder, J. Fontaine, M. Joseph, N. Kauffman, A. Killion, P. Kirchner, A. Lindauer, S. Maple, J. Moore, J. Rosen, and T. Spang). We thank staff at Sequoia-Kings Canyon and Yosemite National Parks (especially D. Boiano and R. Grasso), Inyo and Sierra National Forests, California Department of Fish and Wildlife (especially J. Erdman), U.S. Fish and Wildlife Service, and Sierra Nevada Aquatic Research Laboratory for research permits, logistical support, and/or field assistance. Thanks to J. Dozier for assistance with CDEC data. This project was funded by grants from the National Park Service (to R.A.K.), Yosemite Conservancy (to R.A.K.), National Science Foundation to C.J.B. (EF-0723563, DEB-1557190, DBI-2120084) and to M.Q.W (DEB-2133401), and NIH Grant R01ES12067 (to C.J.B.).

Author contributions

All authors contributed to the conceptual development of the manuscript. Roland Knapp, Cheryl Briggs, and Thomas Smith collected the data. Mark Wilber, Cherie Briggs, and Roland Knapp performed the analyses. Mark Wilber wrote the first draft. All authors contributed to revisions.

Conflict of interest

None

Data availability statement

Code and data are available from Zenodo at `https://zenodo.org/badge/latestdoi/496634407` (Wilber *et al.* 2022)

References

Abatzoglou, J.T. (2013) Development of gridded surface meteorological data for ecological applications and modelling. *International Journal of Climatology*, *33*, 121–131.

Adams, A.J., Kupferberg, S.J., Wilber, M.Q., Pessier, A.P., Grefsrud, M., Bobzien, S., Vredenburg, V.T. & Briggs, C.J. (2017) Extreme drought, host density, sex, and bullfrogs influence fungal pathogen infection in a declining lotic amphibian. *Ecosphere*, *8*, e01740.

Aiello, C.M., Nussear, K.E., Walde, A.D., Esque, T.C., Emblidge, P.G., Sah, P., Bansal, S. & Hudson, P.J. (2014) Disease dynamics during wildlife translocations: Disruptions to the host population and potential consequences for transmission in desert tortoise contact networks. *Animal Conservation*, *17*, 27–39.

Anderson, R.M. & May, R.M. (1979) Population biology of infectious diseases: Part I. *Nature*, *280*, 361 – 367.

Andre, S.E., Parker, J. & Briggs, C.J. (2008) Effect of temperature on host response to *Batrachochytrium dendrobatidis* infection in the mountain yellow-legged frog (*Rana muscosa*). *Journal of Wildlife Diseases*, *44*, 716–720.

Barrile, G.M., Chalfoun, A.D. & Walters, A.W. (2021) Infection status as the basis for habitat choices in a wild amphibian. *The American Naturalist*, *197*, 128–137.

Begon, M., Davis, S., Laudisoit, A., Leirs, H. & Reijniers, J. (2019) Sylvatic plague in Central Asia: a case study of abundance thresholds. K. Wilson, A. Fenton & D. Tompkins, eds., *Wildlife Disease Ecology: Linking Theory to Data and Application*. Cambridge University Press, Cambridge.

Bosch, J., Carrascal, L.M., Manica, A. & Garner, T.W. (2020) Significant reductions of host abundance weakly impact infection intensity of *Batrachochytrium dendrobatidis*. *PLoS ONE*, *15*, e0242913.

Boyle, D.G., Boyle, D.B., Olsen, V., Morgan, J.A.T. & Hyatt, A.D. (2004) Rapid quantitative detection of chytridiomycosis (*Batrachochytrium dendrobatidis*) in amphibian samples using real-time Taqman PCR assay. *Diseases of Aquatic Organisms*, *60*, 141–8.

Bradford, D.F. (1984) Temperature modulation in a high-elevation amphibian, *Rana muscosa*. *Copeia*, *1984*, 966–976.

Briggs, C.J., Knapp, R.A. & Vredenburg, V.T. (2010) Enzootic and epizootic dynamics of the chytrid fungal pathogen of amphibians. *Proceedings of the National Academy of Sciences*, *107*, 9695–9700.

Canessa, S., Ottonello, D., Rosa, G., Salvidio, S., Grasselli, E. & Oneto, F. (2019) Adaptive management of species recovery programs: A real-world application for an endangered amphibian. *Biological Conservation*, *236*, 202–210.

Carpenter, B., Gelman, A., Hoffman, M.D., Lee, D., Goodrich, B., Betancourt, M., Brubaker, M., Guo, J., Li, P. & Riddell, A. (2017) Stan : A probabilistic programming language. *Journal of Statistical Software*, *76*, 1–32.

Courtois, E.A., Loyau, A., Bourgoin, M. & Schmeller, D.S. (2017) Initiation of *Batrachochytrium dendrobatidis* infection in the absence of physical contact with infected hosts - a field study in a high altitude lake. *Oikos*, *126*, 843–851.

Dallas, T.A., Krkošek, M. & Drake, J.M. (2018) Experimental evidence of a pathogen invasion threshold. *Royal Society Open Science*, *5*, 171975.

Davis, S., Leirs, H., Viljugrein, H., Stenseth, N.C., De Bruyn, L., Klassovskiy, N., Ageyev, V. & Begon, M. (2007) Empirical assessment of a threshold model for sylvatic plague. *Journal of the Royal Society Interface*, *4*, 649–657.

De Castro, F. & Bolker, B. (2005) Mechanisms of disease-induced extinction. *Ecology Letters*, *8*, 117–126.

Deredec, A. & Courchamp, F. (2003) Extinction thresholds in host-parasite dynamics. *Annales Zoologic Fennici*, *40*, 115–130.

Diekmann, O., Heesterbeek, J.A.P. & Britton, T. (2013) *Mathematical Tools for Understanding Infectious Disease Dynamics.* Princeton University Press, Princeton.

DiRenzo, G.V., Tunstall, T.S., Ibáñez, R., DeVries, M.S., Longo, A.V., Zamudio, K.R. & Lips, K.R. (2018) External reinfection of a fungal pathogen does not contribute to pathogen growth. *EcoHealth*, *15*, 815–826.

Fischer, J. & Lindenmayer, D.B. (2000) An assessment of the published results of animal relocations. *Biological Conservation*, *96*, 1–11.

Fisher, M.C., Henk, D.A., Briggs, C.J., Brownstein, J.S., Madoff, L.C., McCraw, S.L. & Gurr, S.J. (2012) Emerging fungal threats to animal, plant and ecosystem health. *Nature*, *484*, 186–94.

Frick, W.F., Cheng, T.L., Langwig, K.E., Hoyt, J.R., Janicki, A.F., Parise, K.L., Foster, J.T. & Kilpatrick, A. (2017) Pathogen dynamics during invasion and establishment of white-nose syndrome explain mechanisms of host persistence. *Ecology*, *98*, 624–631.

Gillespie, G.R., Hunter, D., Berger, L. & Marantelli, G. (2015) Rapid decline and extinction of a montane frog population in southern Australia follows detection of the amphibian pathogen *Batrachochytrium dendrobatidis*. *Animal Conservation*, *18*, 295–302.

Golas, B.D., Goodell, B. & Webb, C.T. (2021) Host adaptation to novel pathogen introduction: predicting conditions that promote evolutionary rescue. *Ecology Letters*, *24*, 2238–2255.

Haydon, D.T., Cleaveland, S., Taylor, L.H. & Laurenson, M.K. (2002) Identifying reservoirs of infection: A conceptual and practical challenge. *Emerging Infectious Diseases*, *8*, 1468–1473.

Hopkins, S.R., Fleming-Davies, A.E., Belden, L.K. & Wojdak, J.M. (2020) Systematic review of modelling assumptions and empirical evidence: Does parasite transmission increase nonlinearly with host density? *Methods in Ecology and Evolution*, *11*, 476–486.

Jani, A.J., Knapp, R.A. & Briggs, C.J. (2017) Epidemic and endemic pathogen dynamics correspond to distinct host population microbiomes at a landscape scale. *Proceedings of the Royal Society B*, *284*, 20170944.

Joseph, M.B. & Knapp, R.A. (2018) Disease and climate effects on individuals drive post-reintroduction population dynamics of an endangered amphibian. *Ecosphere*, *9*, e02499.

Kilpatrick, A.M., Briggs, C.J. & Daszak, P. (2010) The ecology and impact of chytridiomycosis: an emerging disease of amphibians. *Trends in Ecology and Evolution*, *25*, 109–118.

Knapp, R.A., Fellers, G.M., Kleeman, P.M., Miller, D.A., Vredenburg, V.T., Rosenblum, E.B. & Briggs, C.J. (2016) Large-scale recovery of an endangered amphibian despite ongoing exposure to multiple stressors. *Proceedings of the National Academy of Sciences*, *113*, 11889–11894.

Knapp, R.A. (2005) Effects of nonnative fish and habitat characteristics on lentic herpetofauna in Yosemite National Park, USA. *Biological Conservation*, *121*, 265–279.

Knapp, R.A. (2021) Exploring an unknown world: under-ice observations of Sierra Nevada alpine lakes in winter. , University of California, Santa Barbara, https://www.youtube.com/watch?v=5PMtsZ3nIIs.

Knapp, R.A., Briggs, C.J., Smith, T.C. & Maurer, J.R. (2011) Nowhere to hide: impact of a temperature-sensitive amphibian pathogen along an elevation gradient in the temperate zone. *Ecosphere*, *2*, art93.

Knapp, R.A. & Matthews, K.R. (2000) Non-native mountain fish introductions and the decline of the mountain yellow-legged frog from within protected areas. *Conservation Biology*, *14*, 428–438.

Knapp, R.A., Matthews, K.R., Preisler, H.K. & Jellison, R. (2003) Developing probabilistic models to predict amphibian site occupancy in a patchy landscape. *Ecological Applications*, *13*, 1069–1082.

Kyle, C.H., Liu, J., Gallagher, M.E., Dukic, V. & Dwyer, G. (2020) Stochasticity and infectious disease dynamics: Density and weather effects on a fungal insect pathogen. *American Naturalist*, *195*, 504–523.

Lande, R., Engen, S. & Saether, B.E. (2003) *Stochastic Population Dynamics in Ecology and Conservation.* Oxford University Press, Oxford.

Lloyd-Smith, J.O., Cross, P.C., Briggs, C.J., Daugherty, M.P., Getz, W.M., Latto, J., Sanchez, M.S., Smith, A.B. & Swei, A. (2005) Should we expect population thresholds for wildlife disease? *Trends in Ecology and Evolution*, *20*, 511–519.

Longcore, J.E., Pessier, A.P. & Nichols, D.K. (1999) *Batrachochytrium dendrobatidis* gen. et sp . nov., a chytrid pathogenic to amphibians. *Mycologia*, *91*, 219–227.

McClintock, B.T., Langrock, R., Gimenez, O., Cam, E., Borchers, D.L., Glennie, R. & Patterson, T.A. (2020) Uncovering ecological state dynamics with Hidden Markov Models. *Ecology Letters*, *23*, 1878–1903.

Merkle, E.C. & Rosseel, Y. (2018) blavaan: Bayesian structural equation models via parameter expansion. *Journal of Statistical Software*, *85*.

Mihaljevic, J.R., Polivka, C.M., Mehmel, C.J., Li, C., Dukic, V. & Dwyer, G. (2020) An empirical test of the role of small-scale transmission in large-scale disease dynamics. *American Naturalist*, *195*, 616–635.

Rachowicz, L.J. & Briggs, C.J. (2007) Quantifying the disease transmission function: effects of density on *Batrachochytrium dendrobatidis* transmission in the mountain yellow-legged frog *Rana muscosa*. *The Journal of Animal Ecology*, *76*, 711–21.

Reeder, N.M.M., Pessier, A.P. & Vredenburg, V.T. (2012) A reservoir species for the emerging amphibian pathogen *Batrachochytrium dendrobatidis* thrives in a landscape decimated by disease. *PLoS ONE*, *7*, e33567.

Reijniers, J., Davis, S., Begon, M., Heesterbeek, J.A., Ageyev, V.S. & Leirs, H. (2012) A curve of thresholds governs plague epizootics in Central Asia. *Ecology Letters*, *15*, 554–560.

Smits, A.P., Gomez, N.W., Dozier, J. & Sadro, S. (2021) Winter climate and lake morphology control ice phenology and under-ice temperature and oxygen regimes in mountain lakes. *Journal of Geophysical Research: Biogeosciences*, *126*, 1–20.

Sonn, J.M., Utz, R.M. & Richards-Zawacki, C.L. (2019) Effects of latitudinal, seasonal, and daily temperature variations on chytrid fungal infections in a North American frog. *Ecosphere*, *10*, e02892.

Tompkins, D.M., Dunn, A.M., Smith, M.J. & Telfer, S. (2011) Wildlife diseases: From individuals to ecosystems. *Journal of Animal Ecology*, *80*, 19–38.

Tompros, A., Dean, A.D., Fenton, A., Wilber, M.Q., Davis, E. & Matthew, C. (2022) Frequency-dependent transmission of *Batrachochytrium salamandrivorans* in eastern newts. *Transboundary and Emerging Diseases*, *69*, 731–741.

Vehtari, A., Gelman, A. & Gabry, J. (2016) Practical Bayesian model evaluation using leave-one-out cross-validation and WAIC. *Statistics and Computing*, pp. 1–20.

Vredenburg, V.T., Knapp, R.A., Tunstall, T.S. & Briggs, C.J. (2010) Dynamics of an emerging disease drive large-scale amphibian population extinctions. *Proceedings of the National Academy of Sciences*, *107*, 9689–94.

Vredenburg, V.T., McNally, S.V., Sulaeman, H., Butler, H.M., Yap, T., Koo, M.S., Schmeller, D.S., Dodge, C., Cheng, T., Lau, G. & Briggs, C.J. (2019) Pathogen invasion history elucidates contemporary host pathogen dynamics. *PLoS ONE*, *14*, e0219981.

Wilber, M.Q., Knapp, R.A., Toothman, M. & Briggs, C.J. (2017) Resistance, tolerance and environmental transmission dynamics determine host extinction risk in a load-dependent amphibian disease. *Ecology Letters*, *20*, 1169–1181.

Wilber, M.Q., Knapp, R.A., Smith, T.C. & Briggs, C.J. (2022) Data from: Host density has limited effects on pathogen invasion, disease-induced declines, and within-host infection dynamics across a landscape of disease. Zenodo. https://zenodo.org/badge/latestdoi/496634407.

Wilber, M.Q., Johnson, P.T.J. & Briggs, C.J. (2019) When chytrid fungus invades: integrating theory and data to understand disease-induced amphibian declines. K. Wilson, A. Fenton & D.M. Tompkins, eds., *Wildlife Disease Ecology: Linking Theory to Data and Application*, chapter 18. Cambridge University Press, Cambridge, United Kingdom.

Wilber, M.Q., Langwig, K.E., Kilpatrick, A.M., McCallum, H.I. & Briggs, C.J. (2016) Integral Projection Models for host-parasite systems with an application to amphibian chytrid fungus. *Methods in Ecology and Evolution*, *7*, 1182–1194.

Zhou, H., Hanson, T. & Knapp, R. (2015) Marginal Bayesian nonparametric model for time to disease arrival of threatened amphibian populations. *Biometrics*, *71*, 1101–1110.

Table 1: ΔLOOIC values for the four models of success and failed invasion fit at different prevalence cutoffs ρ. ΔLOOIC values should only be compared within a column. Lower values indicate a better predictive model. "Full model" indicates the model given in equation 1. All other models are modified relative to the full model.

Model description	**Host abundance or density**	**ΔLOOIC**		
		$\rho = 0.25$	$\rho = 0.33$	$\rho = 0.50$
Full model	abundance	0	0	0
Full model	density	2.74	2.83	0.90
Replace tadpoles p/a with $\log_{10}$ tadpoles	abundance	6.61	7.44	3.78
Replace tadpoles p/a with $\log_{10}$ tadpoles	density	11.12	10.79	3.32
Remove winter severity	abundance	2.30	5.73	4.94
Remove winter severity	density	6.30	8.90	7.12
Remove winter severity, replace linear temperature w/ quadratic temperature	abundance	6.54	9.96	6.42
Remove winter severity, replace linear temperature w/ quadratic temperature	density	9.49	13.24	7.21

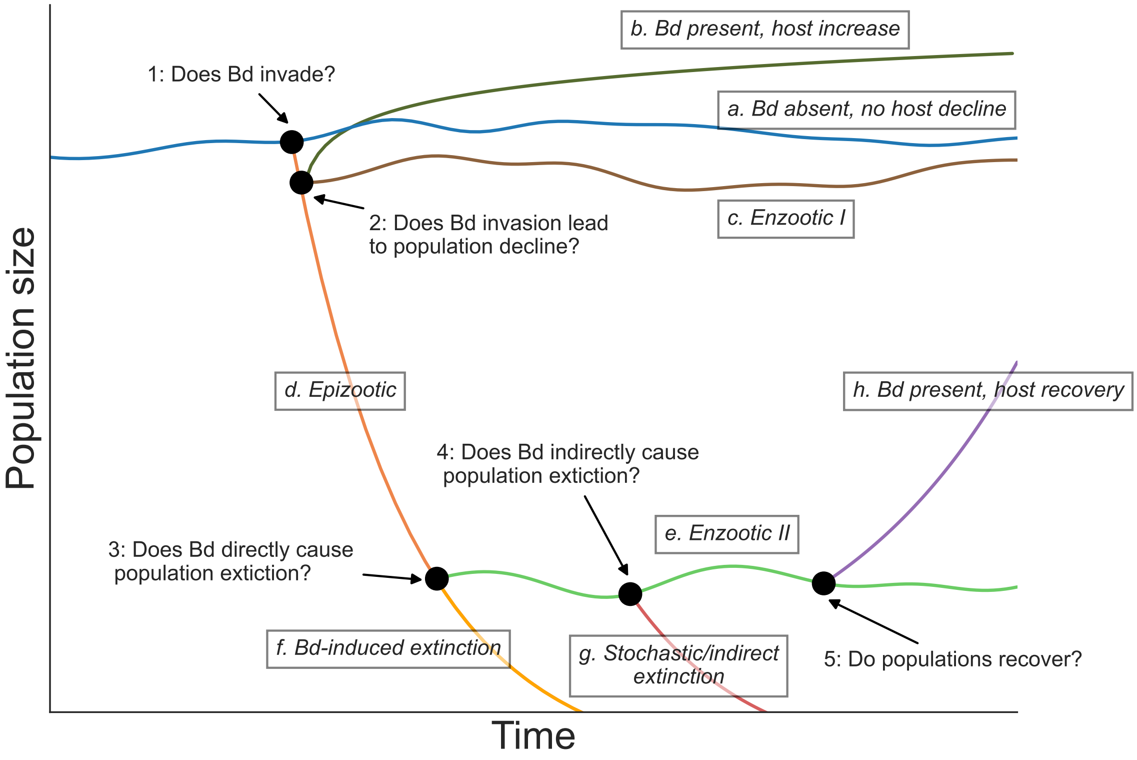

Figure 1: Framework for contextualizing different response trajectories in host-parasite systems, with a particular focus on amphibian populations experiencing infection with *Batrachochytrium dendrobatidis* (*Bd*). The black dots give the five branch points at which the trajectories of host-parasite systems can diverge, leading to variability in response trajectories. The boxes refer to the different population-level trajectories observed in amphibian-*Bd* systems. Reproduced from Wilber *et al.* (2019).

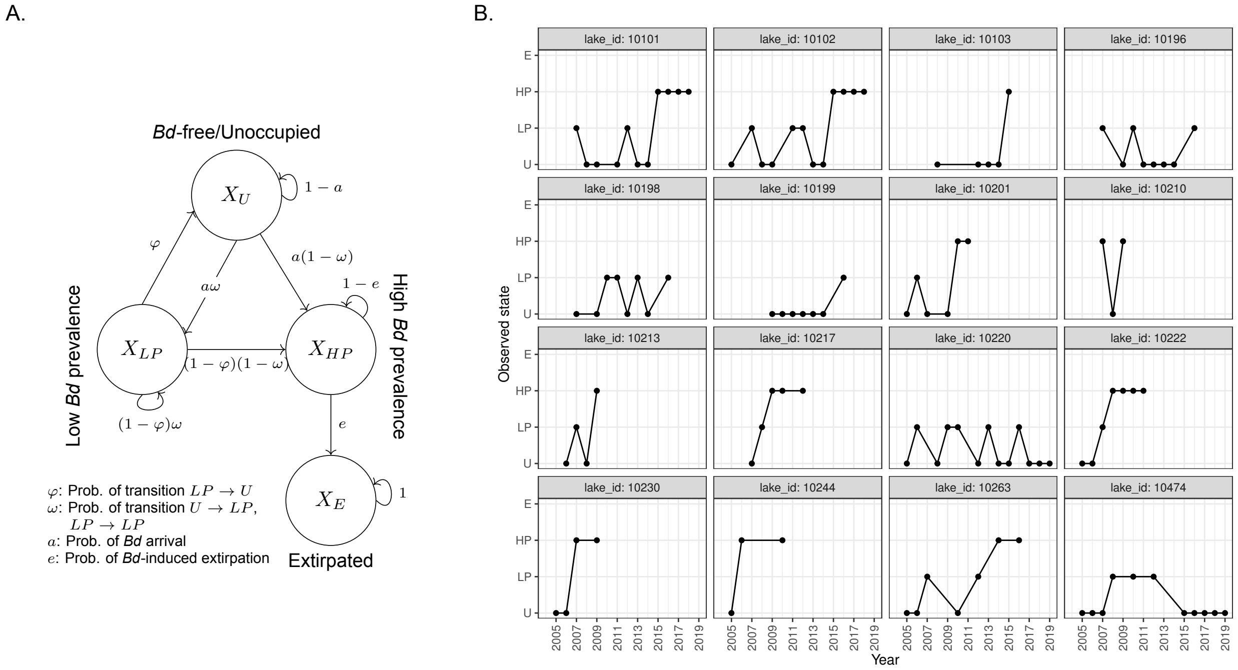

Figure 2: **A.** A directed graph of the state process model used to describe successful and failed invasions in the *R. sierrae*-*Bd* system. The circles represent the four possible states a frog population can take: *Bd*-free/Unoccupied, low *Bd* prevalence, high *Bd* prevalence, and extirpated. The parameters give the transition probabilities among states as described in the main text. **B.** Observed state trajectories from 16 example amphibian populations. In these plots the cutoff between a low prevalence state and a high prevalence state is $\rho = 0.5$. Numbers in facets are unique lake ids.

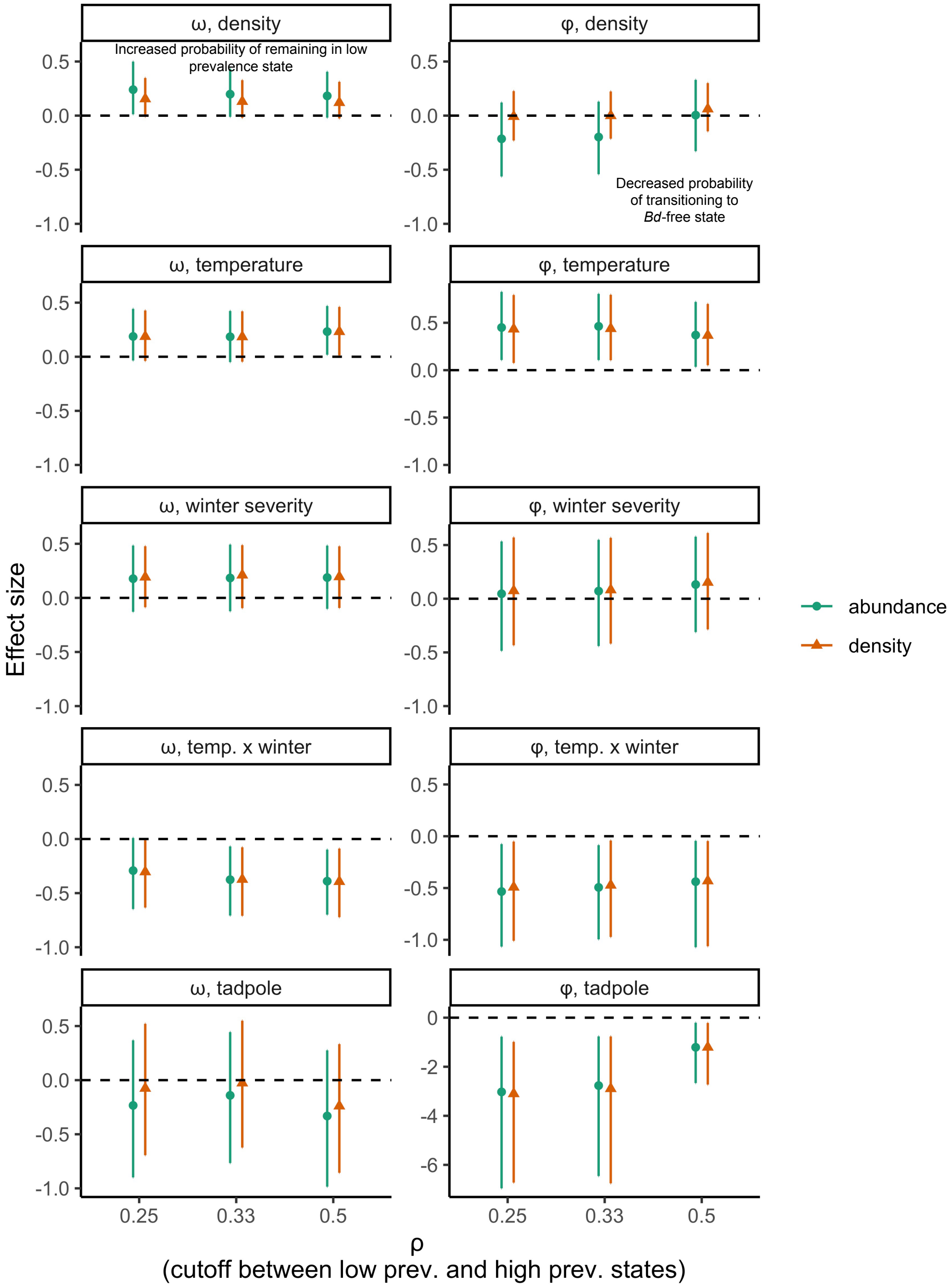

Figure 3: The estimated effect sizes of frog abundance or density, maximum summer temperature, winter severity (snow water equivalents), and tadpole presence/absence on the probability of transitioning from a low prevalence to a *Bd*-free population (φ) and the probability of a *Bd*-invaded population remaining in a low prevalence state rather than transitioning to the high prevalence state (ω). All effect sizes other than tadpole presence/absence are estimated from standardized predictors (subtracting the mean and dividing by the standard deviation). Reported effect sizes are the medians with 95% credible intervals. The dashed line indicates an effect size of zero. Models were fit with different prevalence cutoffs ρ that delineated a low prevalence population (prevalence $< \rho$) from a high prevalence population (prevalence $> \rho$). Parameter estimates are shown for different values of ρ. Points above the dashed line indicate that increasing a covariate increases the given transition probability, and below the dashed line indicate that increasing the covariate decreases the given transition probability. Note that all subplots other than 'φ, tadpole' have the same y-axis.

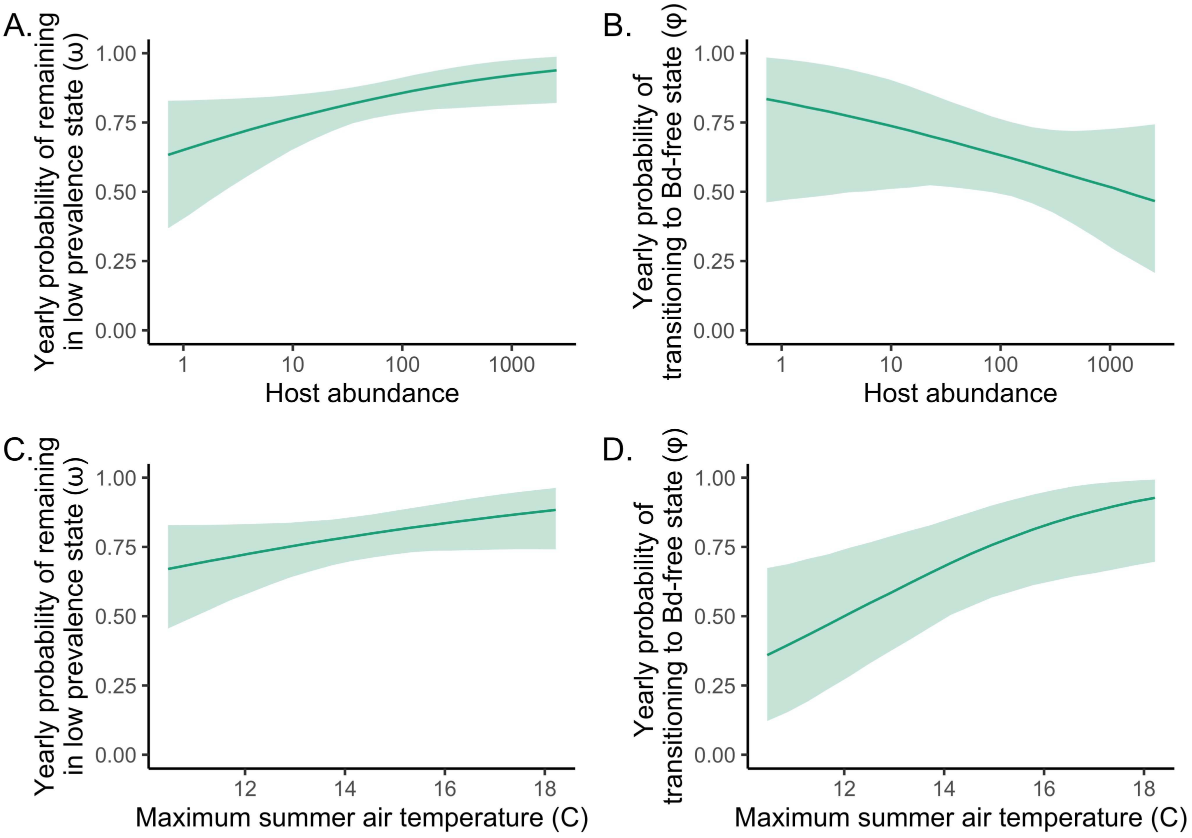

Figure 4: **A., B.** The inferred effects of host abundance on ω and ϕ. **C., D.** The inferred effects of average summer air temperature on ω and ϕ when host abundance is used as a covariate. In all plots, $\rho = 0.25$, lines give the median estimated probabilities when all other covariates in the model are set to their mean values and tadpoles are present (equation 1), and shaded ribbons are 95% credible intervals.

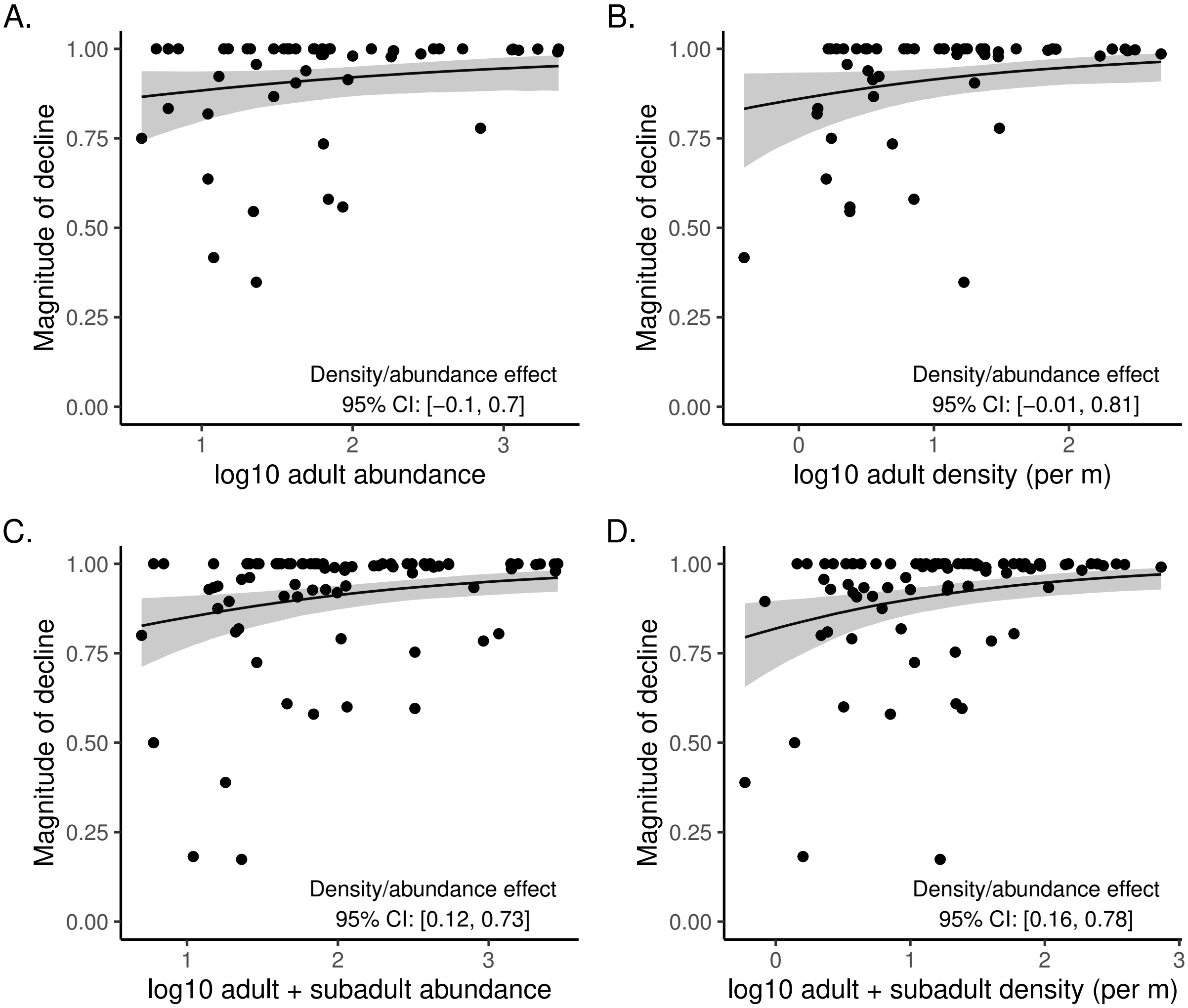

Figure 5: **A.** Observed and predicted magnitudes of amphibian population declines across varying adult abundances prior to *Bd*-induced declines. Black points are the observed magnitudes of population declines (1 - minimum abundance over survey period / maximum abundance over survey period). Black lines are the model predicted relationships between host abundance/density and the magnitude of decline and gray ribbon is the 95% credible interval. **B.** Same as A., but using maximum density of adults. Maximum density is calculated as adult abundance / lake perimeter. **C.** Same as A., but using maximum abundance of adults + subadults. **D.** Same as A., but using maximum density of adults + subadults.

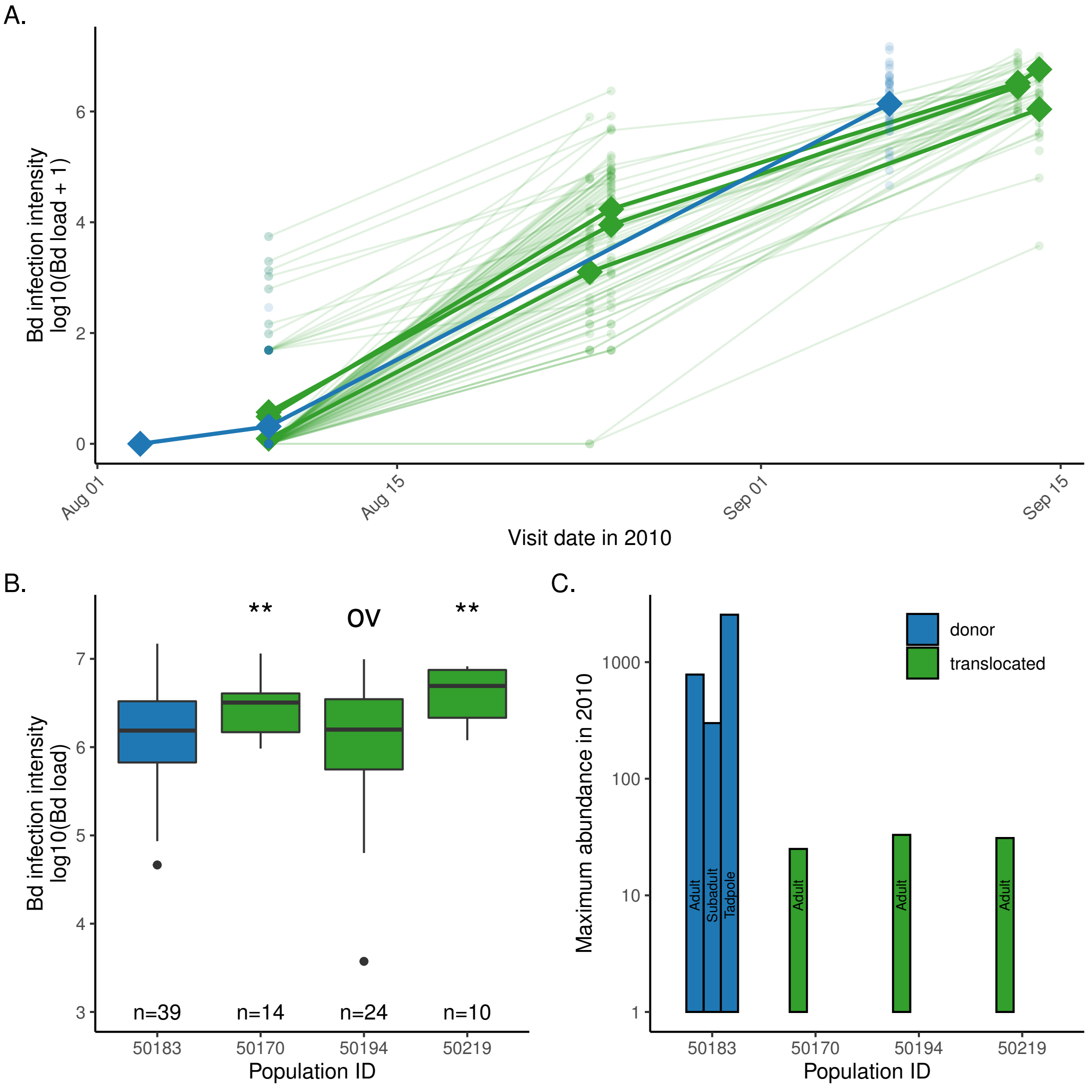

Figure 6: **A.** *Bd* infection intensity data from the frog translocation study. On Aug. 3, 2010, adult frogs from the donor population 50183 were swabbed and identified as *Bd* negative. On Aug. 8, 2010, 120 adult frogs were collected from 50183, pit tagged, swabbed, and moved to three frog-free sites (50170, 50219, and 50194). The translocated populations were surveyed again on Aug. 24-25 and Sept. 13-14. The thick green lines and diamonds show mean infection intensities on frogs that eventually ended up in specific translocated populations (though all frogs were in 50183 prior to Aug. 3). The thick blue line and diamonds show mean infection intensities in the source population 50183 over three sampling events. The thin and partially transparent lines and points show load trajectories for individual frogs. We statistically compared infection data from populations on and after Sept. 8, 2010 in panel B. **B.** Boxplots of infection intensities on frogs in the donor and translocated populations from surveys that took place on or after Sept. 8, 2010. The "**" symbol over boxplots indicate whether the 95% credible interval of the difference between infection intensities in the translocated populations and in the donor population did not overlap zero (i.e., a notable difference). "ov" indicates intervals did overlap zero. Sample sizes show how many swabs are contributing to the estimate of the mean in each population. **C.** The maximum abundance of adults, subadults, and tadpoles observed during 2010 visual encounter surveys. The translocated populations had no frogs immediately prior to translocations and no tadpoles or subadults following translocations. Note that the y-axis is on a log-scale. Plotting the y-axis in units of host density, rather than abundance, does not change the qualitative differences between lakes.